11-2-2015

# Comparison of Microfacet BRDF Model to Modified Beckmann-Kirchhoff BRDF Model for Rough and Smooth Surfaces

Samuel D. Butler
*Air Force Institute of Technology*

Stephen E. Nauyoks
*Air Force Institute of Technology*

Michael A. Marciniak
*Air Force Institute of Technology*



## Recommended Citation

Butler, S. D., Nauyoks, S. E., & Marciniak, M. A. (2015). Comparison of microfacet BRDF model to modified Beckmann-Kirchhoff BRDF model for rough and smooth surfaces. Optics Express, 23(22), 29100. https://doi.org/10.1364/OE.23.029100

# Comparison of microfacet BRDF model to modified Beckmann-Kirchhoff BRDF model for rough and smooth surfaces

**Samuel D. Butler,**[1,*] **Stephen E. Nauyoks,**[1] **and Michael A. Marciniak**[1]

[1]*Department of Engineering Physics, Air Force Institute of Technology, 2950 Hobson Way, Wright-Patterson AFB, OH 45433-7765, USA*

[*]*sbutler@afit.edu*

**Abstract:** A popular class of BRDF models is the microfacet models, where geometric optics is assumed. In contrast, more complex physical optics models may more accurately predict the BRDF, but the calculation is more resource intensive. These seemingly disparate approaches are compared in detail for the rough and smooth surface approximations of the modified Beckmann-Kirchhoff BRDF model, assuming Gaussian surface statistics. An approximation relating standard Fresnel reflection with the semi-rough surface polarization term, $Q$, is presented for unpolarized light. For rough surfaces, the angular dependence of direction cosine space is shown to be identical to the angular dependence in the microfacet distribution function. For polished surfaces, the same comparison shows a breakdown in the microfacet models. Similarities and differences between microfacet BRDF models and the modified Beckmann-Kirchhoff model are identified. The rationale for the original Beckmann-Kirchhoff $F_{bk}^2$ geometric term relative to both microfacet models and generalized Harvey-Shack model is presented. A modification to the geometric $F_{bk}^2$ term in original Beckmann-Kirchhoff BRDF theory is proposed.



**OCIS codes:** (290.1483) BSDF, BRDF, and BTDF; (290.5825) Scattering theory; (290.5835) Scattering, Harvey; (290.5880) Scattering, rough surfaces; (280.0280) Remote sensing and sensors.

## References and links

1. J. R. Schott, *Fundamentals of Polarimetric Remote Sensing* (SPIE, 2009).
2. M. T. Eismann, *Hyperspectral Remote Sensing* (SPIE, 2012).
3. K. E. Torrance and E. M. Sparrow, "Theory of off-specular reflection from roughened surfaces," J. Opt. Soc. Am. **57**, 1105–1114 (1967).
4. J. R. Maxwell, J. Beard, S. Weiner, D. Ladd, and S. Ladd, "Bidirectional reflectance model validation and utilization," Environmental Research Institute of Michigan (ERIM) Technical Report AFAL-TR-73-303 (1973).
5. D. R. Crow, C. F. Coker, D. L. Garbo, and E. M. Olson, "Closed-loop real-time infrared scene generator," Proc. SPIE **3368**, 342 (1998).
6. J. F. Blinn, "Models of light reflection for computer synthesized pictures," in *Proceedings of the 4th Annual Conference on Computer Graphics and Interactive Techniques*, (ACM, 1977), pp. 192–198.
7. R. L. Cook and K. E. Torrance, "A reflectance model for computer graphics," ACM Trans. Graphics **1**, 7–24 (1982).
8. W. Matusik, H. Pfister, M. Brand, and L. McMillan, "A data-driven reflectance model," ACM Trans. Graphics **22**, 759–769 (2003).
9. A. Ngan, F. Durand, and W. Matusik, "Experimental analysis of BRDF models," in *Proceedings of the Eurographics Symposium on Rendering*, (Eurographics Association, 2005) pp. 117–226 (2005).

#244131 Received 6 Jul 2015; revised 1 Sep 2015; accepted 2 Sep 2015; published 29 Oct 2015

10. F. E. Nicodemus, J. C. Richmond, J. J. Hsia, I. W. Ginsberg, and T. Limperis, "Geometrical considerations and nomenclature for reflectance," National Bureau of Standards Monograph 160, Department of Commerce (1977).
11. S. D. Butler and M. A. Marciniak, "Robust categorization of microfacet BRDF models to enable flexible application-specific BRDF adaptation," Proc. SPIE **9205**, 920506 (2014).
12. S. D. Butler, S. E. Nauyoks, and M. A. Marciniak, "Experimental analysis of bidirectional reflectance distribution function cross section conversion term in direction cosine space," Opt. Lett. **40**, 2445–2448 (2015).
13. S. D. Butler, S. E. Nauyoks, and M. A. Marciniak, "Comparison of microfacet BRDF model elements to diffraction BRDF model elements," Proc. SPIE **9472**, 94720C (2015).
14. J. E. Harvey and A. Krywonos, "Unified scatter model for rough surfaces at large incident and scatter angles," Proc. SPIE **6672**, 66720C (2007).
15. A. Krywonos, J. E. Harvey, and N. Choi, "Linear systems formulation of scattering theory for rough surfaces with arbitrary incident and scattering angles," J. Opt. Sci. Am. A **28**, 1121–1138 (2011).
16. G. J. Ward, "Measuring and modeling anisotropic surfaces," in *Proceedings of SIGGRAPH Computer Graphics '92*, (ACM, 1992), 265–272. (1992).
17. A. Duer, "An improved normalization for the Ward reflectance model," J. Graphics, GPU, and Game Tools **11**, 51–59 (2006).
18. M. W. Hyde IV, J. D. Schmidt, and M. J. Havrilla, "A geometrical optics polarimetric bidirectional reflectance distribution function for dielectric and metallic surfaces," Opt. Express **17**, 22138–22153 (2009).
19. R. G. Priest and T. A. Germer, "Polarimetric BRDF in the microfacet model: Theory and measurements," in *Proceedings of 2000 Meeting of the MSS Specialty Sensors Group on Passive Sensors*, (Naval Research Lab, 2000), pp. 169–182.
20. J. D. Jackson, *Classical Electrodynamics*, 3rd ed. (John Wiley and Sons, Inc., 1999).
21. J. Dorsey, H. Rushmeier, and F. Sillion, *Digital Modeling of Material Appearance* (Morgan Kaufmann, 2007).
22. S. Rusinkiewicz, "A new change of variables for efficient BRDF representation," in *Rendering Techniques '98*, (Springer Vienna, 1998), pp. 11–22.
23. R. G. Priest and S. R. Meier, "Polarimetric microfacet scattering theory with applications to absorptive and reflective surfaces," Opt. Eng. **41(5)**, 988–993 (2002).
24. T. S. Trowbridge and K. P. Reitz, "Average irregularity reprentation of a rough surface for ray reflection," J. Opt. Soc. Am. **65**, 531–536 (1975).
25. T. M. Elfouhaily and C.-A. Guerin, "A critical survey of approximate scattering wave theories from random rough surfaces," Waves in Random Media **14**, R1–R40 (2004).
26. S. Chakrabarti, A. A. Maradudin, and E. R. Mendez, "Reconstruction of the surface-height autocorrelation function of a randomly rough dielectric surface from incoherent light scattering," Phys. Rev. A **88**, 013812 (2013).
27. P. Beckmann and A. Spizzichino, *The Scattering of Electromagnetic Waves from Rough Surfaces* (MacMillan, 1963).
28. J. E. Harvey, A. Krywonos, and C. L. Vernold, "Modified Beckmann-Kirchhoff scattering model for rough surfaces with large incident and scattering angles," Opt. Eng. **46(7)**, 078002 (2007).
29. A. Krywonos, "Predicting surface scatter using a linear systems formulation of non-paraxial scalar diffraction," Ph.D. Dissertation, University of Central Florida (2006).
30. J. C. Stover, *Optical Scattering: Measurement and Analysis*, 3rd ed. (SPIE, 2012).
31. J. C. Stover and J. E. Harvey, "Unified scatter model for rough surfaces at large incident and scatter angles," Proc. SPIE **6672**, 66720B (2007).
32. S. Schröder, A. Duparré, L. Coriand, A. Tünnermann, D. H. Penalver, and J. E. Harvey, "Modeling of light scattering in different regimes of surface roughness," Opt. Express **19**, 9820–9835 (2011).
33. E. Heitz, "Understanding the masking-shadowing function in microfacet-based BRDFs," J. Comp. Graph. Tech. **3**, 32–91 (2014).

## 1. Introduction

The bidirectional reflectance distribution function (BRDF) defines the ratio of the reflected radiance to the incident irradiance for materials, and is commonly used in remote sensing [1,2], scene generation [3–5], and computer graphics [6–9]. Nicodemus formally defined the BRDF as [10]

$$f_r = \frac{dL_s(\hat{\omega}_i, \hat{\omega}_s, \lambda)}{dE_i(\hat{\omega}_i, \lambda)}, \tag{1}$$

where $\hat{\omega}_i$ is the incident unit vector and $\hat{\omega}_s$ is the scattered (outgoing) unit vector, where in both cases $\hat{\omega} = [1, \theta, \phi]^T$ is a unit vector pointing in the incident (or scattered) direction, with

#244131 Received 6 Jul 2015; revised 1 Sep 2015; accepted 2 Sep 2015; published 29 Oct 2015

spherical coordinates $\theta$ (representing elevation angle) and $\phi$ (representing azimuthal angle) as measured from the surface normal; see Fig. 1(a). $\lambda$ represents the wavelength of light.

We are interested in using the BRDF to render scenes which are both radiometrically and spectrally accurate, yet are computationally inexpensive to implement. Therefore, in this paper, two different approaches to modeling BRDF will be compared: microfacet model BRDFs and scalar wave optics model BRDFs. The former assumes geometric optics only, but results in several easy-to-use closed-form expressions for the BRDF that can be written in a common form [11]. The latter uses linear systems theory to develop a scalar BRDF based on wave optics, but is much more cumbersome to apply to resource-constrained problems. The purpose of this paper is to understand how the physics of a more complete scalar wave optics model may be related to microfacet closed-form BRDF models. All components of microfacet models are directly related to components of a scalar wave optics model through the development of novel relationships between differing elements in these models. Surface reflection is fundamentally a physical optics problem, but understanding how a closed-form geometric optics model relates to a more complete, but more computationally complex, physical optics model may lead to development of models that are more radiometrically and spectrally accurate for applications that require a closed-form approximation, as is desirable for resource-constrained applications of the BRDF such as remote sensing.

To accomplish this task, first these models are introduced. Then, the rough and smooth surface limits of the wave optics model are compared to the common form used by many microfacet models. Relationships are then developed between the different components of the models, suggesting a different approach to modeling the geometric attenuation (shadowing and masking) term in microfacet models, as well as explaining limitations in microfacet models by quantifying differences in the angular terms in the models. Finally, the relationships developed in this paper are used to explain the role of the original Beckmann-Kirchhoff geometric term as compared to both models, and to explain experimental results in [12]. No BRDF model can be reasonably simple and simultaneously perfect, but comparing the microfacet class of BRDF models to a scalar wave optics model and developing relationships between all components of these models may lead to future development of closed-form BRDF models that correct for deficiencies in microfacet models.

## 2. Background

This section discusses two classes of BRDF models: the microfacet class of models and the Modified Beckmann-Kirchhoff (MBK) scalar wave optics model. These models form the basis of comparison in the remainder of the paper. Prior work in [11–15] has set the stage for comparing the simplicity of a closed-form approximation given by a geometric optics BRDF model with the accuracy of a more robust scalar wave optics model such as MBK BRDF theory. A summary of these key results is presented as background.

### *2.1. Microfacet BRDF models*

The microfacet class of BRDF models includes several popular models, such as Torrance-Sparrow [3], Blinn-Phong [6], Cook-Torrance [7], Ward-Duer [16, 17], Hyde [18], Priest-Germer [19], and Beard-Maxwell [4]. These microfacet models for isotropic surfaces can all be written in a general form as [11]

$$f_\mu(\hat{\omega}_i,\hat{\omega}_s) = \rho_s F(\theta_d) D_\mu(\theta_h) G(\hat{\omega}_i,\hat{\omega}_s)\sigma(\theta_i,\theta_s) + \rho_v V(\hat{\omega}_i,\hat{\omega}_s) + \rho_d/\pi, \tag{2}$$

where the first group of terms is due to surface reflection, the second to volumetric scattering $V$, and the third to Lambertian scattering. $\rho_s$, $\rho_v$, and $\rho_d$ are fit parameters that are allowed

#244131 Received 6 Jul 2015; revised 1 Sep 2015; accepted 2 Sep 2015; published 29 Oct 2015

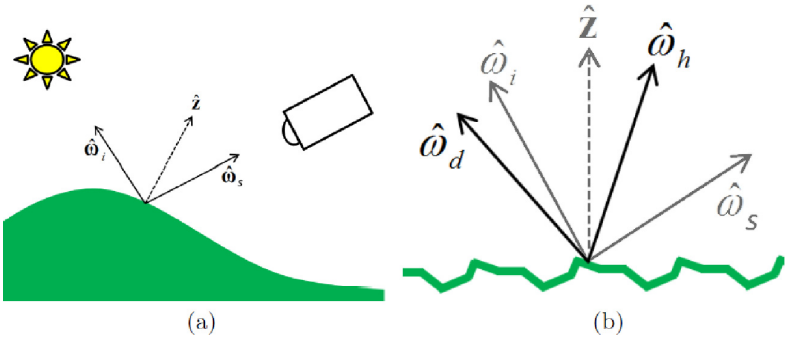


Fig. 1. Relevant coordinate systems for the microfacet (geometric) BRDF model. (a) BRDF coordinate system orientation relative to the surface normal $\hat{\mathbf{z}}$. (b) Microfacet coordinates relative to the coordinates defined in (a). In all cases, $\hat{\omega}$ has a $\theta$ and $\phi$ component in spherical coordinates, and is normalized to a magnitude of 1 [11].

to vary with wavelength and signify the amount of surface, volume, and diffuse (Lambertian) reflectance for a material. For surface-reflecting materials in a single bounce model, $\rho_v = 0$ and $\rho_d = 0$. $F$ is the Fresnel reflectance as derived in many optics and electromagnetism textbooks such as [20], with the usual parameters of complex refractive index $\tilde{n} = n + i\kappa$. $D_\mu$ is the microfacet surface normal statistical distribution. $G$ is a geometric attenuation (shadowing and masking) term. $\sigma$ is a conversion from scattering cross section to BRDF, defined as

$$\sigma(\theta_i, \theta_s) = \frac{1}{4\cos\theta_i \cos\theta_s}. \tag{3}$$

Overviews of popular microfacet models are given in [11, 21]. In this paper, all surfaces are assumed to be isotropic; $\phi_i = 0$ is chosen as the orientation of the $\phi$ axis. Microfacet coordinates $\theta_h$ (representing the half angle, or angle of the bisector) and $\theta_d$ (representing the incident angle in the microfacet's frame of reference) have been used since the Torrance-Sparrow BRDF in 1967 [3], but were only recently formally defined as [22]

$$\begin{aligned} \hat{\omega}_h &= \frac{\hat{\omega}_i + \hat{\omega}_s}{||\hat{\omega}_i + \hat{\omega}_s||}, \\ \hat{\omega}_d &= \mathbb{R}_y(-\theta_h)\mathbb{R}_z(-\phi_h), \end{aligned} \tag{4}$$

where $\mathbb{R}_a$ is a rotation about some axis $a$. This formal definition has the advantage of specifying the $\phi$ dependence of $\hat{\omega}_h$ and $\hat{\omega}_d$ in addition to the $\theta$ dependence, which is of particular importance for anisotropic surfaces. In the isotropic case, only the $\theta_h$ and $\theta_d$ angles are computed using equations that appear in many papers in microfacet literature [3, 4, 7, 16, 18, 19, 23], and are given as

$$\cos(2\theta_d) = \cos\theta_i \cos\theta_s + \sin\theta_i \sin\theta_s \cos\phi_s, \tag{5}$$

$$\cos\theta_h = \frac{\cos\theta_i + \cos\theta_s}{2\cos\theta_d}. \tag{6}$$

The Gaussian distribution $D_g$ is used in the Torrance-Sparrow [3], Cook-Torrance [7], Ward-Duer [16, 17] (in the small angle approximation), Priest-Germer [19], and Hyde [18] BRDF models as well as being approximated by the popular cosine lobe distribution used in Blinn-Phong [6], and is given by [11]

#244131 Received 6 Jul 2015; revised 1 Sep 2015; accepted 2 Sep 2015; published 29 Oct 2015

$$D_g(\theta_h) = \frac{1}{2\pi\sigma_g^2 \cos^4\theta_h} \exp\left[-\frac{\tan^2\theta_h}{2\sigma_g^2}\right], \tag{7}$$

where $\sigma_g$ is commonly thought of as statistically describing the microfacet orientation, but is actually a fit parameter which will be shown here to vary with wavelength, indicating a breakdown of the geometric optics model. From geometric optics, $\sigma_g$ represents the probability distribution of microsurface normals. Mathematically, the microfacet surface normal probability distribution can be calculated from the surface height profile by calculating the normal to the derivative of the surface height profile. The angular dependence of the distribution function is primarily driven by $\tan^2\theta_h$. The remaining terms, and in particular the $1/\cos^4\theta_h$ term, normalize the Gaussian distribution to ensure it is a proper probability distribution function in projected area (as Trowbridge indicates is the proper normalization in [24]); that is,

$$\int_0^{2\pi}\int_0^{\pi/2} D_g(\theta_h)\cos\theta_h \sin\theta_h \, d\theta_h \, d\phi_h = 1. \tag{8}$$

Unlike linear systems models, the closed-form expression for microfacet models presented in Eq. (2) is used for both very rough and smooth surfaces.

### *2.2. Modified Beckmann-Kirchhoff model*

Several different physical optics models have been developed, deriving from the Kirchhoff tangent plane approximation, small perturbation approximation, and other unifying methods; for a 2004 survey of over 30 of these models, see [25]. Elfouhaily noted all of these models had deficiencies. Krywonos then developed Generalized Harvey-Shack (GHS) theory and MBK theory to correct some of these deficiencies.

More recently, a method for estimating surface statistics using the tangent plane approximation and assuming a Gaussian distribution of surface properties was developed in [26]. Although this method did not include out-of-plane scatter, its success in predicting surface statistics lends credence to using a physical optics model based on the tangent plane approximation, which is used by the Beckmann-Kirchhoff (BK) scattering model.

The BK scattering model was formulated in 1963 [27]. Similar to [26], the BK model uses the tangent plane approximation and assumes a Gaussian distribution of surface properties. However, the original BK theory was formulated prior to formal definition of the BRDF in 1977 [10]. This BK model was modified when the linear systems diffraction BRDF theory was generalized to all incident and scattered angles, as well as for a variety of surfaces, by Krywonos [15]. Linear systems diffraction BRDF theory was originally formulated for paraxial reflection in the Harvey-Shack BRDF model, then was extended to arbitrary angles in the GHS BRDF model [14, 15, 28]. The GHS BRDF model developed by Krywonos does not possess a known closed-form solution in general. GHS theory is more physically rigorous, but is more computationally intensive and unfortunately, this method fails to distinguish between scattering due to surface reflection versus scattering due to volumetric effects. In both cases, the surface is treated as adding an overall phase offset, regardless of whether the scatter is due to the surface or due to impurities in the material. Krywonos also proposed MBK BRDF theory in [15, 28, 29] that is equal to his GHS theory in the limit of either a polished or very rough surface [28, 29]. This formulation assumes Gaussian statistics, but results in an infinite series expression for the BRDF that more readily enables comparison to the microfacet class of models without sacrificing the accuracy of the GHS model, from which the modifications to the original BK theory were derived.

In GHS and MBK theory, the BRDF is calculated in direction cosine space $(\alpha, \beta)$ instead of spherical space $(\theta, \phi)$. This space is defined as

#244131 Received 6 Jul 2015; revised 1 Sep 2015; accepted 2 Sep 2015; published 29 Oct 2015

$$\begin{aligned}\Delta\alpha &= \alpha_s - \alpha_i = \lambda\, \nu_y = \sin\theta_s \sin(\phi_s - \pi) \\ \Delta\beta &= \beta_s - \beta_i = \lambda\, \nu_x = \sin\theta_s \cos(\phi_s - \pi) - \sin\theta_i,\end{aligned} \tag{9}$$

where the extra $\pi$ terms here arise from a difference in defining the $\phi = 0$ location in the microfacet model as compared to the linear systems model. For in-plane forward scatter, $\phi_s = \pi$ in both models as presented here (backscatter is $\phi_s = 0$); however, in-plane forward scatter data is represented by $\phi_s = 0$ in some linear systems papers [14, 15]. For isotropic samples, the angular dependence simplifies to

$$\eta_r^2 = (\Delta\alpha)^2 + (\Delta\beta)^2 = \sin^2\theta_i + \sin^2\theta_s + 2\sin\theta_i \sin\theta_s \cos\phi_s = \left(\frac{\lambda\, \nu_{xy}}{2\pi}\right)^2, \tag{10}$$

where $\nu_{xy}$ is the notation used by Beckmann [27].

The MBK formulation presented in Eq. (11) is the Angle Spread Function (ASF), $f_a$, which is related to the radiance $L$; the ASF is equal to the BRDF if $F = 1$ (total Fresnel reflectance). Assuming the surface statistics follow a Gaussian autocovariance, and taking into account the $1/\lambda^2$ term present in MBK as shown in [29], the ASF is calculated as

$$f_a = \frac{\pi K l_c^2}{\lambda^2} \exp(-g) \sum_{m=1}^{\infty} \frac{g^m}{m!m} \exp\left(-\frac{\nu_{xy}^2 l_c^2}{4m}\right), \tag{11}$$

where $K$ is a renormalization term that ensures conservation of energy, $l_c$ is the correlation length of the surface, and $g$ is related to the surface height $\sigma_s$ and given as [28]

$$g(\theta_i, \theta_s) = \left(\frac{2\pi\sigma_s}{\lambda}\right)^2 (\cos\theta_i + \cos\theta_s)^2. \tag{12}$$

When written in terms of scattered radiance $L_s$, $K$ is defined as [15, 28, 29]

$$K(\beta_i) = \frac{\int_{-\infty}^{\infty}\int_{-\infty}^{\infty} L_s(\alpha_s, \beta_s - \beta_i)\, d\beta_s\, d\alpha_s}{\int_{-1}^{1}\int_{-\sqrt{1-\alpha_s^2}}^{\sqrt{1-\alpha_s^2}} L_s(\alpha_s, \beta_s - \beta_i)\, d\beta_s\, d\alpha_s}. \tag{13}$$

$L_s \geq 0$ everywhere, so $K \geq 1$ for all incident angles. Physically, $K$ is a unitless quantity that ensures energy is not lost to evanescent waves by redistributing energy that may fall outside the unit circle of real space defined by the direction cosines. For some BRDF applications, this term can be problematic to compute because it depends on knowing the surface distribution shape, and involves computation of a double integral expression that does not possess an analytic solution for most surface distributions.

For a smooth surface, $\sigma_s << \lambda$ and as such only the $m = 1$ term of the sum in Eq. (11) is significant. In [29], Krywonos defines a smooth surface as $g(\theta_i, \theta_s) < 0.025$, which results in less than 1% error compared to the infinite series summation when $\theta_i \leq 70°$. By using Eqs. (10)-(12) and multiplying by the polarization factor $Q$ to convert the ASF to a BRDF, this polished approximation $f_p$ can be written as

$$f_p = \frac{4\pi^3 l_c^2 \sigma_s^2 Q(\cos\theta_i + \cos\theta_s)^2}{\lambda^4} \exp\left[-\left(\frac{\pi l_c \eta_r}{\lambda}\right)^2\right], \tag{14}$$

where $\exp(-g) \approx 1$ since $\sigma_s << \lambda$ for a polished surface, and $K \approx 1$ for a polished surface, as shown in [15].

At the other extreme, if a surface is very rough, the BRDF $f_{vr}$ as given in [29] can be rewritten using Eqs. (10)-(12) as

#244131 Received 6 Jul 2015; revised 1 Sep 2015; accepted 2 Sep 2015; published 29 Oct 2015

$$f_{vr} = \frac{KQl_c^2}{4\pi\sigma_s^2(\cos\theta_i+\cos\theta_s)^2}\exp\left[-\left(\frac{l_c}{2\sigma_s}\right)^2\left(\frac{\eta_r}{\cos\theta_i+\cos\theta_s}\right)^2\right], \tag{15}$$

where again we have multiplied by the polarization factor $Q$ to convert from ASF to BRDF. In [29], Krywonos defines very rough as $g(\theta_i,\theta_s) > 800$, to result in less than 1% maximum error as compared to the infinite summation when $\theta_i \leq 70^\circ$.

The appropriate Fresnel term to convert ASF to BRDF is the polarization factor $Q$ as described by Stover in [30]. The more popular unpolarized Fresnel reflectance term $F$ derived in many electromagnetism and optics texts assumes plane wave incidence and an infinitely smooth surface. The derivation of the polarization factor $Q$ in [30] relaxes the infinite plane wave and perfectly smooth assumptions in the derivation of $F$. For *s*-polarized light incident on a surface, $Q_s = Q_{ss} + Q_{sp}$. For *p*-polarized light incident on a surface, $Q_p = Q_{ps} + Q_{pp}$. For unpolarized light incident on a surface, $Q = Q_s + Q_p$. If $\theta_i = \theta_s$ and $\phi_s = 180^\circ$ (specular reflection), the equations for $Q_s$ and $Q_p$ reduce to the standard Fresnel equations $F_s$ and $F_p$.

In [15, 31], careful measurements of material surface statistics were made by Stover. The measured surface statistics were used to compute the Power Spectral Density (PSD) of each surface. Stover then measured the BRDF of these surfaces. The GHS BRDF model was used to compute the PSD from the BRDF data. The computed PSD using GHS theory closely matched the measured surface statistics of the surfaces. Similarly, in [32], Schröder *et al.* used GHS theory to predict the scatter off an arbitrary (but known) surface of arbitrary roughness, both rough and smooth. Since GHS matches MBK in the very rough or very smooth approximation, $f_p$ and $f_{vr}$ from MBK theory are considered to be accurate physical models in the limit of a polished or very rough surface, respectively.

## 3. Analysis

To compare these BRDF models, the ratio of microfacet BRDFs to the MBK BRDF is taken in both the very rough approximation and the smooth surface approximation, assuming an isotropic sample. We also assume surface statistics (surface height and autocorrelation length) follow a Gaussian distribution.

Since MBK theory can be used to predict accurate surface statistics, the ratios $f_\mu / f_p$ and $f_\mu / f_{vr}$ would equal 1 if the microfacet model also modeled physical truth. Differences from 1 indicate deviations in the microfacet model from the more physical MBK model, and may suggest how to alter the microfacet model to improve its accuracy while still maintaining a closed-form approximation to the BRDF.

### 3.1. *Very rough surface comparison*

The ratio of microfacet BRDFs $f_\mu$ to the very rough surface MBK BRDF $f_{vr}$ is

$$\begin{aligned}\frac{f_\mu}{f_{vr}} = \left(\frac{\rho_s}{2K}\right)\left(\frac{2FG}{Q}\right)\left(\frac{(\cos\theta_i+\cos\theta_s)^2}{4\cos\theta_i\cos\theta_s\cos^4\theta_h}\right)\left(\frac{\sigma_s\sqrt{2}}{l_c\sigma_g}\right)^2 \times \\ \exp\left[-\left(\frac{\tan^2\theta_h}{2\sigma_g^2} - \frac{l_c^2}{4\sigma_s^2}\frac{\eta_r^2}{(\cos\theta_i+\cos\theta_s)^2}\right)\right].\end{aligned} \tag{16}$$

The exponential term will be analyzed first. The angular dependence is contained in two terms: $\tan^2\theta_h$ from the microfacet model and $\eta_r^2/(\cos\theta_i+\cos\theta_s)^2$ from MBK. Although these terms were derived with a completely different physical interpretation (geometric optics versus physical optics), it will be shown here that these terms are equal at all incident and scattered

#244131 Received 6 Jul 2015; revised 1 Sep 2015; accepted 2 Sep 2015; published 29 Oct 2015

angles, in-plane and out-of-plane. Starting with Eq. (6) and using basic trigonometry identities to rewrite $\cos\theta_h$ in terms of $\tan\theta_h$:

$$\tan^2\theta_h = \frac{4\cos^2\theta_d - (\cos\theta_i + \cos\theta_s)^2}{(\cos\theta_i + \cos\theta_s)^2}. \tag{17}$$

The denominator already matches the denominator of $\eta_r^2/(\cos\theta_i + \cos\theta_s)^2$, so we only need to show that the numerator equals $\eta_r^2$ as given by Eq. (10). This is performed by use of the double angle formula for $\cos(2\theta_d)$ and adding zero:

$$\begin{aligned} 4\cos^2\theta_d - (\cos\theta_i + \cos\theta_s)^2 &= 2 + 2(2\cos^2\theta_d - 1) - (\cos\theta_i + \cos\theta_s)^2 \\ &= 2 + 2\cos(2\theta_d) - (\cos\theta_i + \cos\theta_s)^2 \\ &= \sin^2\theta_i + \cos^2\theta_i + \sin^2\theta_s + \cos^2\theta_s + 2\cos(2\theta_d) - (\cos\theta_i + \cos\theta_s)^2 \\ &= \sin^2\theta_i + \sin^2\theta_s + 2\sin\theta_i\sin\theta_s\cos\phi_s = \eta_r^2, \end{aligned} \tag{18}$$

where in the last line Eq. (5) was used to obtain $\eta_r^2$. Thus, we have shown that linear systems direction cosine space for a very rough surface is exactly equal to the geometric microfacet model bisector space:

$$\tan^2\theta_h = \left(\frac{\eta_r}{\cos\theta_i + \cos\theta_s}\right)^2. \tag{19}$$

The angular term in the exponential from the scalar wave optics model, $\eta_r^2/(\cos\theta_i + \cos\theta_s)^2$, ranges from 0 to $\infty$. This is in contrast to the result obtained later in this paper when examining a polished surface. (The angular term in the exponential from the microfacet model, $\tan^2\theta_h$, always ranges from 0 to $\infty$.)

From geometric optics $\sigma_g$ is commonly thought of as the Gaussian width of the probability distribution of microsurface normals. Mathematically, the microfacet surface normals can be calculated from the surface height profile and is related to the normal to the derivative of the surface height profile; however, only the probability distribution of the surface profile is specified. Instead, from Eq. (16), we solve for $\sigma_g$ for a very rough surface using the remaining terms in the exponential, obtaining

$$\sigma_{g,vr} = \frac{\sigma_s\sqrt{2}}{l_c}. \tag{20}$$

Recall $\sigma_s$ represents the width of the Gaussian in the vertical (height) direction and $l_c$ represents the width of the Gaussian in the horizontal (correlation length) direction. This result is identical to the result obtained in the Hyde polarized BRDF model's parameterization of the Gaussian distribution given in [18] that was derived using the Method of Moments, suggesting the methodology employed in this comparison is correct. However, Eq. (20) only holds for the very rough surface approximation. A different result for the polished surface analysis is obtained later in the paper in Eq. (25), showing this interpretation of $\sigma_g$ is only valid for very rough surfaces, and is not true in general. This point will be discussed in more depth after comparing the polished surface approximation to the microfacet model.

Equation (16) has now simplified to

$$\frac{f_\mu}{f_{vr}} = \left(\frac{\rho_s}{2K}\right)\left(\frac{2FG}{Q}\right)\left(\frac{(\cos\theta_i + \cos\theta_s)^2}{4\cos\theta_i\cos\theta_s\cos^4\theta_h}\right). \tag{21}$$

Direct comparisons between $Q$ and $F$ vary significantly in magnitude. Stover explains the $s$ polarization, but does not suggest an approximation valid at all angles and indices of refraction

#244131 Received 6 Jul 2015; revised 1 Sep 2015; accepted 2 Sep 2015; published 29 Oct 2015

for the $p$ polarization (and thus the unpolarized term $Q = Q_s + Q_p$), although he does present approximations for a few limiting cases [30]. To improve on this understanding, the polarization factor $Q$ was analyzed from the perspective of comparing it to not only Fresnel reflectance, but also to the remaining angular terms from the microfacet model, since the microfacet model uses $F$ instead of $Q$.

In [13], we discovered that, for in-plane angles, there is an approximate relationship $S$ between the unpolarized Fresnel reflectance and the polarization factor, $Q$, given as

$$S = \frac{4\cos\theta_i \cos\theta_s \cos^4\theta_h}{(\cos\theta_i + \cos\theta_s)^2} \approx \frac{2F}{Q}, \tag{22}$$

where the factor of 2 arises from $Q = Q_s + Q_p = F_s + F_p = 2F$ if $\theta_i = \theta_s$ and $\phi_s = 180^\circ$ (standard Fresnel reflection). However, in [13], there was not a solid basis for this approximation. In this paper, the rationale for Eq. (22) is now evident, as this relationship explicitly appears in Eq. (21).

In [13], we also only examined the in-plane relationship. In this paper, a more complete analysis is performed by computing the relative difference between $2F/Q$ and $S$, including at out-of-plane angles, where the relative difference is defined as

$$R_d = \frac{|2F/Q - S|}{2F/Q}. \tag{23}$$

Figure 2 was created at $\theta_i = (15^\circ, 30^\circ, 45^\circ, 60^\circ)$ for five different indices of refraction. For each angle, the five different indices of refraction were chosen to represent a wide range of materials: high $n$ and high $\kappa$: $\tilde{n} = 4 + 10i$; low $n$ and low (but nonzero) $\kappa$: $\tilde{n} = 1.5 + i$, low $n$ and zero $\kappa$: $\tilde{n} = 1.4$, moderate $n$ and $\kappa$: $\tilde{n} = 1.7 + 5i$, and $n < 1$: $\tilde{n} = 0.25 + 3i$. When $\theta_i = \theta_s$ and $\phi_s = 180^\circ$ (specular reflection), $R_d = 0$. In general, even out-of-plane, the error is relatively small if $\theta_i$ and $\theta_s$ are both small, but increases when either $\theta_i$ or $\theta_s$ is large. This result suggests that the cross section conversion term $\sigma(\theta_i, \theta_s)$ in Eq. (3) and the microfacet distribution normalization $1/\cos^4\theta_h$ in Eq. (7) both arise from using $F$ instead of $Q$.

This result also suggests a novel interpretation for $G$. In geometric optics, $G = 1$ when the incident and scattered angles are both small–that is, there is no shadowing and masking. This is consistent with the low relative difference observed in Fig. 2 at small incident and scattered angles. However, the relative difference at large angles does not agree with a geometric optics interpretation. Since the BRDF is fundamentally a wave optics problem, better approximations for $G$ may be derived by solving $2FG/Q = S$ for $G$ instead of from the geometric optics approach detailed in [33]; such a solution is beyond the scope of this paper. Alternatively, $Q$ does have a closed-form solution (although it is substantially more complex than $F$). For increased accuracy, $Q/2$ could be used in place of $F$ using this observed relationship.

### *3.2. Polished surface comparison*

Much of the detail for a similar analysis of $f_\mu/f_p$ in the polished surface approximation is contained in [13], where the microfacet model was compared to GHS. However, GHS was shown to reduce to MBK in the polished surface approximation [15]. Key points from that analysis are presented here.

The ratio $f_\mu/f_p$ results in

#244131 Received 6 Jul 2015; revised 1 Sep 2015; accepted 2 Sep 2015; published 29 Oct 2015

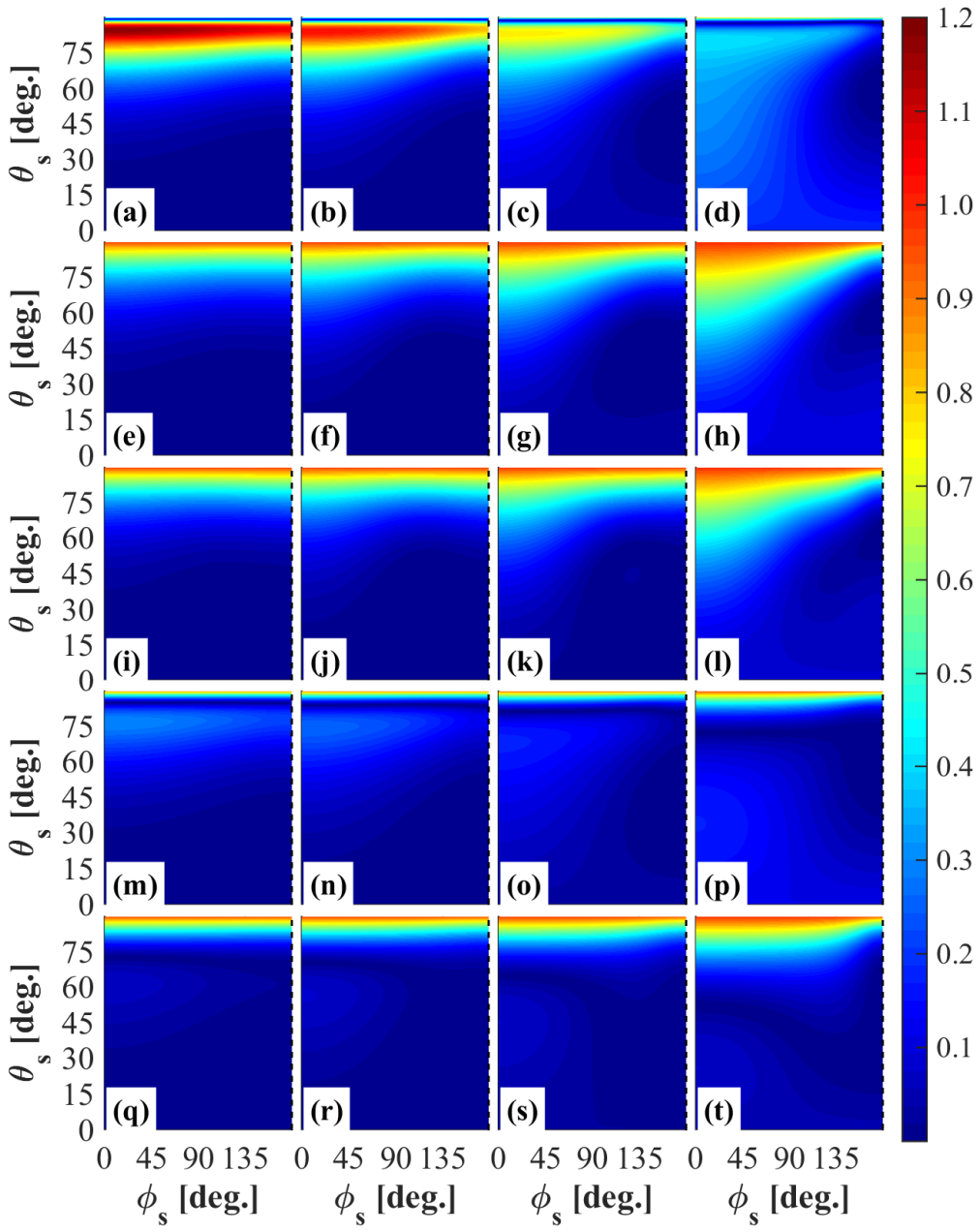


Fig. 2. Surface plot of relative difference $R_d$ for five different indices of refraction: (a-d) $\tilde{n} = 4 + 10i$, (e-h) $\tilde{n} = 1.5 + i$, (i-l) $\tilde{n} = 1.4$, (m-p) $\tilde{n} = 1.7 + 5i$, (q-t) $\tilde{n} = 0.25 + 3i$. For each index, four different incident angles are plotted: (a,e,i,m,q) $\theta_i = 15^\circ$; (b,f,j,n,r) $\theta_i = 30^\circ$; (c,g,k,o,s) $\theta_i = 45^\circ$; (d,h,l,p,t) $\theta_i = 60^\circ$. The plots are all symmetric about $\phi_s = 180^\circ$. The dotted black line at $\phi_s = 180^\circ$ on the right side of each plot represents in-plane scatter. In each case, $R_d = 0$ when $\theta_i = \theta_s$ and $\phi_s = 180^\circ$; $R_d$ is generally small when $\theta_i$ and $\theta_s$ are small.

#244131 Received 6 Jul 2015; revised 1 Sep 2015; accepted 2 Sep 2015; published 29 Oct 2015

$$\frac{f_\mu}{f_p} = \left(\frac{\rho_s \lambda^2}{8\pi^2 \sigma_s^2}\right)\left(\frac{2FG}{Q}\right)\left(\frac{1}{4\cos\theta_i \cos\theta_s \cos^4\theta_h (\cos\theta_i + \cos\theta_s)^2}\right) \times \left(\frac{\lambda^2}{2\pi^2 \sigma_g^2 l_c^2}\right) \exp\left[-\left(\frac{\tan^2\theta_h}{2\sigma_g^2} - \frac{\pi^2 l_c^2 \eta_r^2}{\lambda^2}\right)\right]. \tag{24}$$

Compared to the very rough surface approximation, the angular dependence of the exponential terms has changed, so the microfacet angular dependence is no longer equal to the wave optics angular dependence. From Eq. (19), instead of the exponential from scalar wave optics having an angular dependence of $\tan^2\theta_h$, the angular dependence is $\eta_r^2 = (\tan^2\theta_h)(\cos\theta_i + \cos\theta_s)^2$. Unlike with the very rough surface, the polished surface angular term in the exponential from scalar wave optics, $\eta_r$, only ranges from 0 to 4, not from 0 to $\infty$, but the microfacet model angular term, $\tan^2\theta_h$, still ranges from 0 to $\infty$. Additionally, a different relationship for $\sigma_g$ is observed, given as

$$\sigma_{g,p} = \frac{\lambda}{\pi l_c \sqrt{2}}, \tag{25}$$

which varies with wavelength, unlike in Eq. (20). This shows the microsurface normal interpretation in the microfacet model does not hold for a polished surface, since the microsurface normal distribution should not vary with wavelength.

When making this substitution for $\sigma_g$, it is observed that $\rho_s$ remains a unitless quantity, but varies with surface height and wavelength; that is, $\rho_s \propto \sigma_s^2/\lambda^2$. Additionally, by applying Eq. (22) to substitute for $2F/Q$, it becomes apparent that there remains a $(\cos\theta_i + \cos\theta_s)^{-4}$ term in the ratio, suggesting the microfacet model would be multiplied by a $(\cos\theta_i + \cos\theta_s)^4$ term.

Since there is now a wavelength dependence both in the distribution function and in $\rho_s$, it becomes apparent that a geometric optics model is not suited for this regime. Furthermore, the angular dependence is no longer simply $\tan^2\theta_h$, but now is $\eta_r$. Equation (19) does relate the two expressions, but since the two are not equal, the microfacet model does not appear to be suitable for fitting to polished surfaces, unless corrections for the differences noted here were present.

### *3.3. Original Beckmann-Kirchhoff modification*

In the original BK theory, $F_{bk}^2$ was used instead of $K$, and was described as a geometrical term [27]. Although Krywonos used $K$ in place of $F_{bk}^2$ in MBK, $F_{bk}^2$ is much simpler to compute and may be desirable in some applications of BRDF if a more complete understanding of its role were developed. That purpose is explored in this section. This geometrical factor $F_{bk}^2$ was given as [27]

$$F_{bk}^2 = \left(\frac{1 + (\cos\theta_i \cos\theta_s + \sin\theta_i \sin\theta_s \cos\phi_s)}{\cos\theta_i (\cos\theta_i + \cos\theta_s)}\right)^2. \tag{26}$$

$F_{bk}$ is not to be confused with Fresnel reflectance; it represents a geometric term that does not depend on index of refraction. Its connection to the microfacet model was not clear from prior work on MBK in [27, 28]; in this section, we develop an explanation and a minor modification for this term. Rewriting $F_{bk}^2$ in microfacet coordinates $\theta_h$ and $\theta_d$:

$$F_{bk}^2 = \frac{\cos^2\theta_d}{\cos^2\theta_i \cos^2\theta_h}. \tag{27}$$

Using basic trigonometric manipulations to put $S$ in microfacet coordinates, this term can be rewritten as

#244131 Received 6 Jul 2015; revised 1 Sep 2015; accepted 2 Sep 2015; published 29 Oct 2015

$$\frac{1}{S} = \frac{\cos^2\theta_d}{\cos\theta_i \cos\theta_s \cos^2\theta_h} \approx \frac{Q}{2F}. \tag{28}$$

These equations suggest the purpose of $F_{bk}^2$ is to approximate $Q/2$ so that when BK theory is multiplied by the Fresnel equation $F$, it scales approximately correctly. However, there is an issue with $F_{bk}^2$ as presented. When $\theta_i \neq \theta_s$, $F_{bk}^2$ does not obey Helmholtz reciprocity and differs from this approximation for $Q/2F$. For this reason, we propose using $1/S$ rather than the original $F_{bk}^2$ term; using $1/S$ makes the term functionally equivalent to the cross section conversion and microfacet distribution normalization, with the modified angular term that arises from $g$ in MBK.

### *3.4. BRDF scaling by $1/\sigma$*

In [12], experimentally measured BRDF data was presented in direction cosine space, which aligns BRDF data at all incident angles, other than differing in height. We observed that multiplying measured BRDF data by a term inspired by the microfacet cross section conversion, $\cos\theta_i \cos\theta_s$, resulted in an approximate height alignment. With the $1/S$ term written in microfacet coordinates above,the scaling in direction cosine space that was observed experimentally in [12] can be explained. When at the specular peak, $\cos\theta_h = 1$ ($\theta_h = 0$). Near the specular peak, $\theta_h$ is small and thus $\cos\theta_h \approx 1$. Thus, $S \approx \cos\theta_i \cos\theta_s$ as was observed in [12] to be the scaling term that aligned the BRDF magnitude data in direction cosine space.

## 4. Conclusion

The terms of the MBK BRDF model are now compared to microfacet models, enabling the MBK model to be rewritten in microfacet coordinates (assuming Gaussian statistics) for a very rough surface ($g > 800$) as

$$f_{vr} = \frac{KFG}{4\cos\theta_i \cos\theta_s} \left(\frac{l_c^2}{2\pi\sigma_s^2 \cos^4\theta_h}\right) \exp\left[-\left(\frac{l_c}{2\sigma_s}\right)^2 \tan^2\theta_h\right], \tag{29}$$

and for a polished surface ($g < 0.025$),

$$\begin{aligned} f_p = &\frac{(2\pi)^3 FG(\cos\theta_i + \cos\theta_s)^4}{4\cos\theta_i \cos\theta_s \cos^4\theta_h} \left(\frac{\sigma_s^2 l_c^2}{\lambda^4}\right) \times \\ &\exp\left[-\left(\frac{\pi l_c}{\lambda}\right)^2 \tan^2\theta_h (\cos\theta_i + \cos\theta_s)^2\right]. \end{aligned} \tag{30}$$

The infinite summation can also be written in microfacet coordinates as

$$\begin{aligned} f_{MBK} = &\frac{\pi FG(\cos\theta_i + \cos\theta_s)^2 K l_c^2}{2\lambda^2 \cos\theta_i \cos\theta_s \cos^4\theta_h} \exp(-g) \times \\ &\sum_{m=1}^{\infty} \frac{g^m}{m!m} \exp\left(-\frac{l_c^2}{4m\lambda^2} \tan^2\theta_h (\cos\theta_i + \cos\theta_s)^2\right), \end{aligned} \tag{31}$$

where $g$ is defined in Eq. (12). In this form, a direct comparison between the microfacet class of BRDF models given in Eq. (2) is now possible, which is expected to lead to more physical closed-form BRDF models for applications such as remote sensing and computer graphics.

To obtain the necessary relationships that were used to obtain the above form for the MBK model in microfacet coordinates, and to better comprehend what the microfacet model represents, the very rough surface approximation of MBK was compared to the general form of the

#244131 Received 6 Jul 2015; revised 1 Sep 2015; accepted 2 Sep 2015; published 29 Oct 2015

microfacet model. In the rough surface approximation, the angular dependence of MBK (and thus also of GHS) was shown to be exactly equal to the angular dependence in the microfacet distribution function. The remaining angular terms were compared to the ratio of the standard Fresnel term with the polarization factor $Q$. This led to a novel approximation for $Q$, and suggested where certain terms present in the microfacet BRDF models arise. In particular, part of the microfacet distribution function normalization and the cross section conversion term were found to result from using standard unpolarized Fresnel reflectance $F$ instead of the polarization factor $Q$. The approximation was found to be relatively accurate, except when $\theta_i$ or $\theta_s$ is large; in the microfacet model, this region is where there would be significant shadowing and masking. Since the BRDF is fundamentally a physical optics problem, this observation suggests that instead of attempting to derive the shadowing and masking term from geometric optics, better results may be obtained by developing a modification to the ratio $2F/Q$, particularly at large incident or scattered angles. Alternatively, it is now possible to modify the microfacet model to use $Q$ instead of $F$ using this relationship.

Next, key differences between the polished surface analysis that were detailed in [13] and the rough surface analysis developed in this paper are presented. This resulted in a modification to the angular and wavelength dependencies in the microfacet model for a polished surface, and showed the breakdown of a geometric model for BRDF.

Additionally, the original BK geometric term $F_{bk}^2$ was analyzed, developing an explanation for this term relative to both the microfacet and linear systems models. A modification to $F_{bk}^2$ in the BK model was also proposed. The physical insight developed in this paper is expected to lead to future development of better closed-form approximations to the BRDF that preserve the relative simplicity of the microfacet model, while increasing the fidelity of the microfacet BRDF approximation.

**Acknowledgment**

We would like to thank the United States Air Force Research Laboratory, Sensors Directorate, for supporting this research. The views expressed in this paper are those of the authors and do not necessarily reflect the official policy or position of the United States Air Force, the U. S. Department of Defense, or the U. S. government.

#244131 Received 6 Jul 2015; revised 1 Sep 2015; accepted 2 Sep 2015; published 29 Oct 2015